Appl Nanosci (2016) 6:653–658
DOI 10.1007/s13204-015-0478-7

ORIGINAL ARTICLE

Green hydrothermal synthesis and optical properties of γ-Gd_2S_3 nanoparticles

Sonika Khajuria[1] · Jigmet Ladol[1] · Sumit Sanotra[1] · Haq Nawaz Sheikh[1]

Received: 18 March 2015 / Accepted: 26 June 2015 / Published online: 8 July 2015

Abstract Green synthesis of γ-Gd_2S_3 nanoparticles was carried out using low-temperature hydrothermal route in autoclave. A 1:1 mixture of ionic liquid 1-ethyl-3-methylimidazolium ethyl sulfate, ([EMIM][EtSO4]), and water was used as a solvent. Synthesized nanoparticles were characterized by x-ray powder diffraction (XRPD), scanning electron microscopy (SEM), UV–visible spectroscopy (UV–vis), particle size by dynamic light scattering (DLS) technique, and photoluminescence (PL) studies. XRPD suggests cubic Th_3P_4-type structure for obtained Gd_2S_3 nanoparticles. The size of synthesized nanoparticles is about 86 nm. Optical band gap for these nanoparticles estimated from electronic spectrum is 2.95 eV which shows blue shift from values reported for bulk Gd_2S_3 due to pronounced quantum mechanical effect. These nanoparticles show sharp emission peak at 385 nm and a broad shoulder at 475 nm when excited at 260 nm.

Keywords Rare earth sesquisulfide · γ-Gd_2S_3 · Nanoparticles · Hydrothermal synthesis · Optical band gap · Photoluminescence

Introduction

Synthesis and characterization of rare earth chalcogenides have attracted considerable attention of researchers due to their excellent properties and wide applications in various technological areas, such as optical devices, electrical, catalytic, and biological imaging (Huber et al. 1997; Dekker et al. 2004; Wang et al. 2006; Kong et al. 2007). Over the past few decades, rare earth sesquisulfides (Ln_2S_3, Ln = rare earth) with a cubic Th_3P_4-type structure have captured much attention owing to their high temperature thermoelectric properties (Beaudry et al. 1995). Rare earth sesquisulfides (Ln_2S_3) are known to have three polymorphic forms; α, β, and γ (Grzechnik et al. 1999). Among these γ-form is most studied for promising applications as optoelectronics (Krichevtsov et al. 2001), piezoelectric transducers (Luguev et al. 2000; Gadzhiev et al. 2001; Grzechnik et al. 2001; Qiu et al. 1996; Witz et al. 1996), and optical materials in IR transmission windows (Li et al. 2011). For gadolinium sesquisulfides (Gd_2S_3), α- phase is low-temperature phase, which transforms into γ-phase with increase in temperature. The γ-phase is stable at high temperature and crystallizes in Th_3P_4-type cubic system (space group $I\ 43d$). A significant difference in vapor pressure between rare earth metals and sulfur leads to difficulty in the preparation of rare earth sulfides. However, huge efforts are devoted to develop methods for the preparation of these materials.

So far, researchers have not paid enough attention to the synthesis of these sesquisulfides at nanoscale. Wang et al. (2005) have successfully synthesized γ-Gd_2S_3 by ultrasonic spray pyrolysis. Ohta et al. (2009) have reported synthesis of Ln_2S_3 (Ln = La and Gd) by sulfurization of Ln_2O_3 during thermal decomposition of NH_4SCN. Prashar et al. (2010) have reported low-temperature synthesis of gadolinium monosulfide (GdS) nanoparticles and their pathogen capture efficiency. Nanosized materials have a larger surface area and the quantum mechanical effects such as 'quantum size effect' begins to play a significant role (Shi et al. 2003; Zhang et al. 2005; Kuang et al. 2003; Kim et al. 2004; Markovich et al. 1999). Since properties

✉ Haq Nawaz Sheikh
hnsheikh@rediffmail.com

[1] Department of Chemistry, University of Jammu, Baba Sahib Ambedkar Road, Jammu Tawi, Jammu 180 006, India

of nanoparticles are highly dependent on their structure, size, and morphology, changes in concentration, temperature, and solvents are found to play a critical role in controlling the size-dependent properties.

In the recent past, ionic liquids (ILs) have been used as medium for synthesis of inorganic nano materials (Antonietti et al. 2004; Zhou et al. 2005). Ionic liquids are the salts which are liquid over a wide temperature range. They possess unique characteristics of negligible vapor pressure, wide liquid range, thermal stability, and high ionic conductivity. Ionic liquids have received much attention as 'green' recyclable alternatives to traditional organic solvents. Ionic liquid-assisted synthesis of nanostructures by different synthetic techniques has been reported (Jiang and Zhu 2005; Jiang et al. 2005; Zhu et al. 2004; Jiang et al. 2006; Ge et al. 2010; Behboudnia et al. 2008). Ionic liquids have also been found to show considerable effect on the morphology of nanoparticles.

To the best of our knowledge, there is no report on the synthesis and characterization techniques for gadolinium sesquisulfide nanoparticles at low temperature. In the present work, we report simple ionic liquid-assisted hydrothermal synthesis of unique Gd_2S_3 nanoflowers. Polyvinylpyrrolidone (PVP) has been used as capping agent to stabilize and modify the structural and morphological properties of nanoparticles.

Experimental details

Materials

Gadolinium nitrate $Gd(NO_3)_3{\cdot}6H_2O$ was obtained from Alfa Aesar. Polyvinylpyrrolidone (PVP) and thiourea (NH_2CSNH_2) were obtained from Sigma Aldrich. All the chemicals were of analytical grade and were used without further purification. The used ionic liquid [EMIM][$EtSO_4$] was purchased from Alfa Aesar. Doubly distilled water was used for preparing aqueous solutions.

Synthesis

In a typical procedure, 1 mmol of $Gd(NO_3)_3{\cdot}6H_2O$ (0.451 g), was dissolved in 12 mL of 1:1 solution of ionic liquid [EMIM][$EtSO_4$] and water. To this solution, 3 mmol of thiourea (0.228 g) and 0.2 g of PVP were added while stirring. The solution was kept under stirring for 30 min. The clear solution obtained was then transferred in a 23 mL Teflon-lined stainless steel autoclave, sealed and maintained at 180 °C for 8 h in an electric oven. The autoclave was then cooled to room temperature naturally. The product was collected by centrifugation and washed several times with water and absolute ethanol. The sample was then dried at 70 °C for 2 h and was collected for further characterization.

Characterization techniques

XRPD patterns were recorded from 20° to 65° on a Rigaku Miniflex diffractometer using monochromatic CuKα radiations (The Woodlands, TX, USA). Scanning electron micrographs (SEM) were recorded on Jeol T-300 scanning electron microscope with gold coating (Tokyo, Japan). The UV–Visible absorption spectrum of the sample was recorded on T90 + UV/Vis Spectrophotometer (PG instruments Ltd). The particle size was determined by DLS technique using Zetasizer Nano ZS-90 (Malvern Instruments Ltd., Worcestershire, UK). The photoluminescence excitation and emission spectra were recorded at room temperature using Agilent Cary Eclipse Fluorescence Spectrophotometer equipped with Xenon lamp that was used as excitation source.

Results and discussion

XRD analysis

The phase and crystallinity of as-prepared sample were determined from X-ray powder diffraction pattern. Figure 1 shows the XRPD pattern of γ-Gd_2S_3 nanoparticles. Nanoparticles produce highly intense X-ray diffraction indicating that nanoparticles are crystalline in nature. As evident from the figure, all the diffraction peaks (211), (220), (310), (400), (420), (442), (510), and (440) can be indexed to as well-crystallized single γ-Gd_2S_3 phase (JCPDS: 26-1424). The crystallite size of the nanocrystals

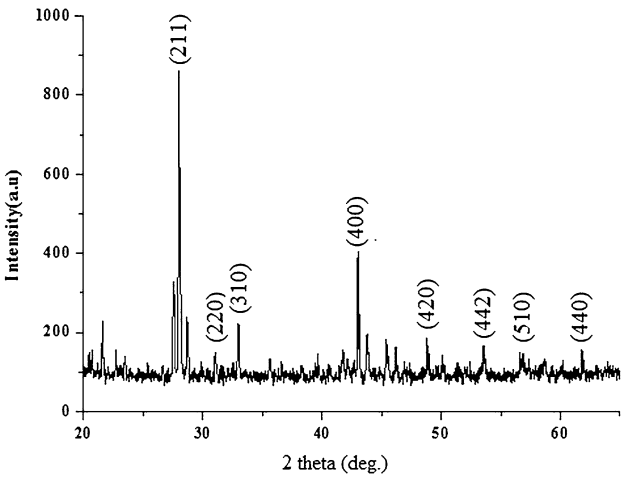

Fig. 1 XRPD pattern for as synthesized γ-Gd_2S_3 nanoparticles

was determined using the well-known Debye–Scherrer's equation given by,

$$D = k\lambda/\beta\cos\theta, \quad (1)$$

where D is the mean grain size, k is the shape factor = 0.94, λ (wavelength of X-rays) = 1.5418 Å for Cu-Kα, β is full width at half maximum (FWHM) of diffraction peaks, and θ is diffraction angle. The average diameter of the grains estimated according to the Scherrer equation [Eq. (1)] is 86 nm.

In order to distinguish the effect of crystallite size and strain on induced broadening, Williamson-Hall plot [Eq. (2)] of XRD profile has been drawn (Williamson et al. 1953). The crystallite size and strain can be obtained from the intercept at y-axis and the slope of line, respectively.

$$\beta_{hkl}\cos\theta = K\lambda/D + 4\varepsilon\sin\theta, \quad (2)$$

where β is FWHM in radian, D is the grain size in nm, ε is the strain, and λ is X-ray wavelength in nanometers. The grain size and strain have been found 71 nm and 2.93×10^{-4} respectively, for γ-Gd_2S_3 nanoparticles.

SEM analysis

The morphology of synthesized γ-Gd_2S_3 nanoparticles was determined by SEM. Typical SEM images of the synthesized nanoparticles at different magnifications are shown in Fig. 2a, b. As depicted from high magnification SEM image (Fig. 2a), the nanoparticles have cuboidal plates like structure. These nanoplates then assemble to produce a flower-like morphology as an evident from low magnification SEM image (Fig. 2b).

UV–visible analysis

The optical property and band gap of γ-Gd_2S_3 nanoparticles were studied using absorption spectrum. For recording the absorption spectrum of γ-Gd_2S_3 nanoparticles, the sample was dispersed in water by using ultrasonic washing for 10 min. The UV–Visible spectrum of γ-Gd_2S_3 nanoparticles is shown in Fig. 3. The synthesized γ-Gd_2S_3 nanoparticles show an absorption at about 420 nm. The absorption refers to the transition of electrons from the valence band to conduction band, and the band gap is the energy difference (in electron volts) between the top of the valence band (E_{vb}) and bottom of the conduction band (E_{cb}). The optical band gap was calculated using equation:

$$E_g(\text{eV}) = hc/\lambda,$$

where λ = wavelength in nm, h = planck's constant, and c = velocity of light.

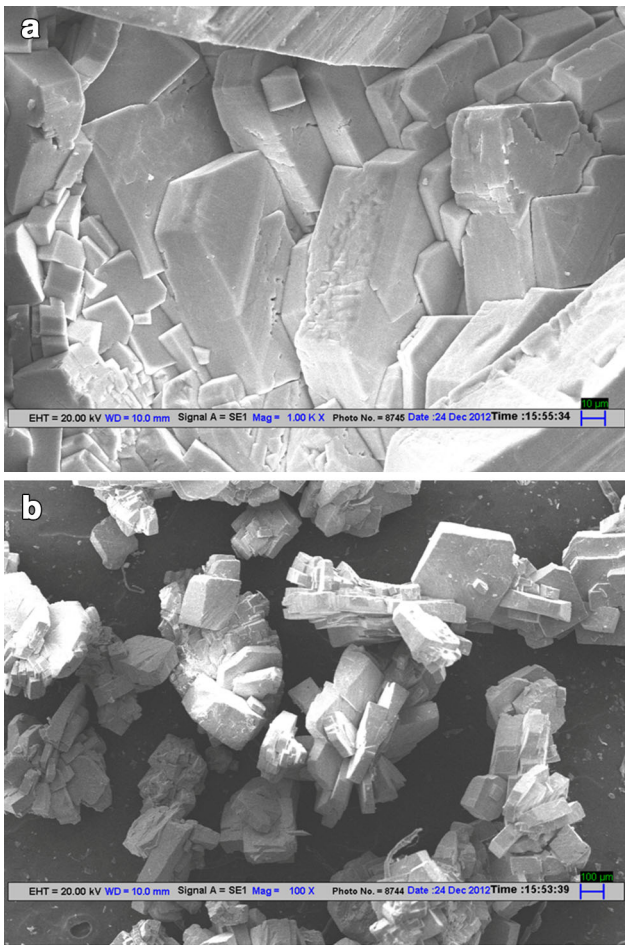

Fig. 2 **a** High magnification SEM image for γ-Gd_2S_3 nanoparticles. **b** Low magnification SEM image for γ-Gd_2S_3 nanoparticles

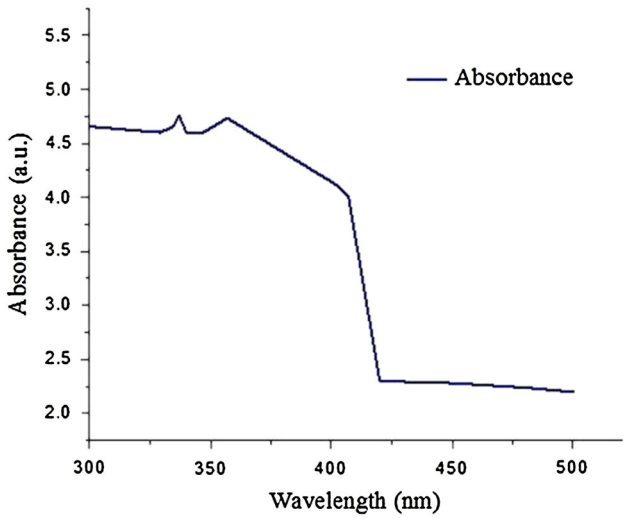

Fig. 3 UV–visible spectrum for γ-Gd_2S_3 nanoparticles

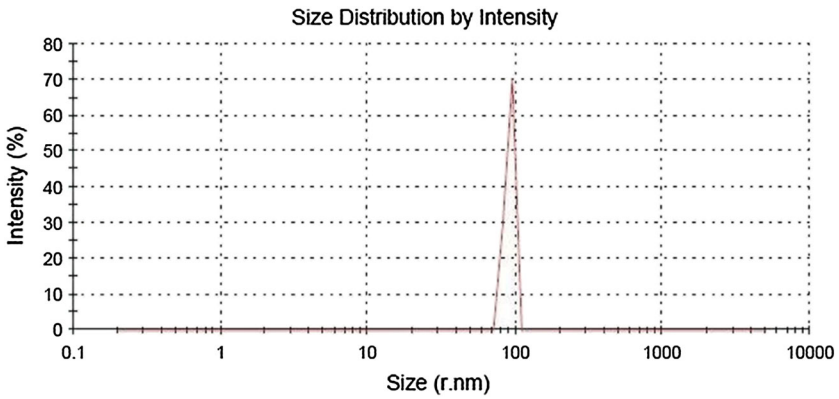

Fig. 4 Particle size by DLS technique for γ-Gd_2S_3 nanoparticles

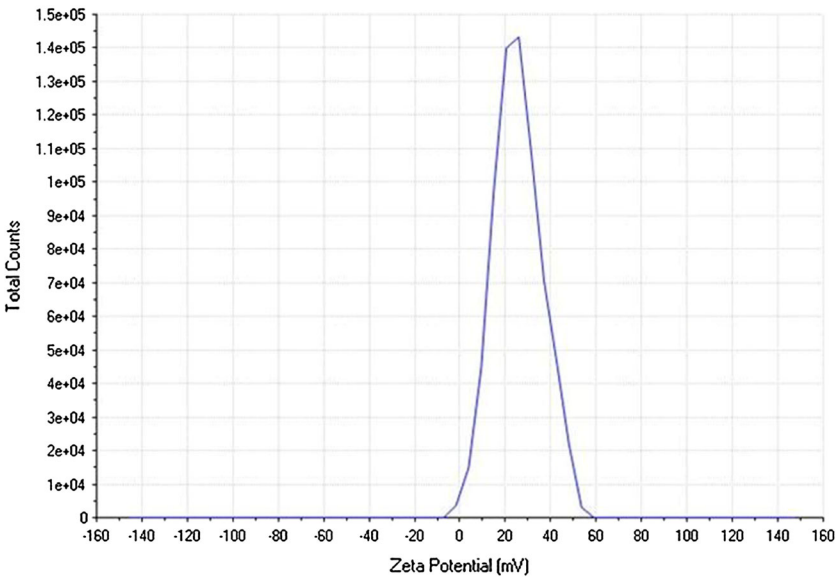

Fig. 5 Zeta potential analysis for γ-Gd_2S_3 nanoparticles

It is found that the optical band gaps of most rare earth sesquisulfides depend on their crystal structures. Furthermore, for the synthetic rare earth sulfides, optical band gap is found in the range of 1.65–3.75 eV. The smallest optical band gap value of 1.65 eV and the largest value of 3.75 eV were obtained for EuS and ε-Lu_2S_3, respectively (Haibin et al. 2009). A band gap of 2.63 eV and 2.93 eV is recorded for γ-Gd_2S_3 by Haibin et al. (2009) and Xixian et al. (2012), respectively. The band gap for synthesized γ-Gd_2S_3 nanoparticles could be estimated at 2.95 eV which is closer to the reported literature. The band gap of as-prepared sample shows the blue shift which might be due to pronounced quantum confinement effect on the nanoparticles.

Particle size by DLS technique

The particle size distribution of synthesized γ-Gd_2S_3 nanoparticles was studied by dynamic light scattering (DLS) technique. The nanoparticles were uniformly dispersed in aqueous medium by mild sonication for 10 min before DLS analysis. The average particle size distribution of synthesized γ-Gd_2S_3 nanoparticles is shown in Fig. 4. The particle size by DLS was found to be 91 nm which is in close agreement with the particle size (86 nm) obtained by Debye–Scherrer method.

Zeta potential measurement

The magnitude of the zeta potential is predictive of the colloidal stability. Nanoparticles with Zeta Potential values greater than +25 mV or less than −25 mV typically have high degrees of stability. The zeta potential analysis of synthesized nanoparticles was carried out by dynamic light scattering (DLS) technique. The nanoparticles were dispersed in methanol by sonication for 10 min to obtain monodisperse solution. For the synthesized nanoparticles, the value of zeta potential was found +25.5 mV which

indicates greater stability of nanoparticles in solution. Figure 5 shows the zeta potential for the synthesized nanoparticles.

Photoluminescence studies

Photoluminescent properties of as-prepared gadolinium sesquisulfide were evaluated on the basis of emission and excitation spectra registered under ultraviolet excitation at room temperature. Figure 6 displays excitation and emission spectra of γ-Gd_2S_3 nanoflowers recorded at room temperature. The emission spectrum shows a sharp emission peak centered at 385 nm accompanied by a broad shoulder at 475 nm, when sample was excited at 260 nm. The sharp emission peak at 385 nm lies in ultraviolet region and is attributed to V_{Gd} defects, and the broad emission peak at 475 nm lies in visible region and can be associated with V_S defects (Xixian et al. 2012). Xixian et al. (2012) have reported that pure γ-Gd_2S_3 nanoparticles synthesized by the thermolysis of precursor complex $Gd[S_2CN(C_4H_8)]_3$·phen show strong emission at 286 and 396 nm, when excited at 243 nm.

In general, purity in color of materials can be recognized by means of color coordinates. Hence, in our present work, the chromaticity coordinates of γ-Gd_2S_3 nanoflowers have been calculated from the emission spectrum by using the commission international De I'Eclairage (CIE) system. The CIE chromaticity diagram for γ-Gd_2S_3 nanoflowers upon excitation at 260 nm is shown in Fig. 7. The CIE coordinate is found to be (0.127, 0.088) which lies within the blue region. The blue color is attributed to broad peak at 475 nm. Therefore, it may be concluded that synthesized γ-Gd_2S_3 nanoflowers can serve as a blue color producing material for display applications and light-emitting diodes.

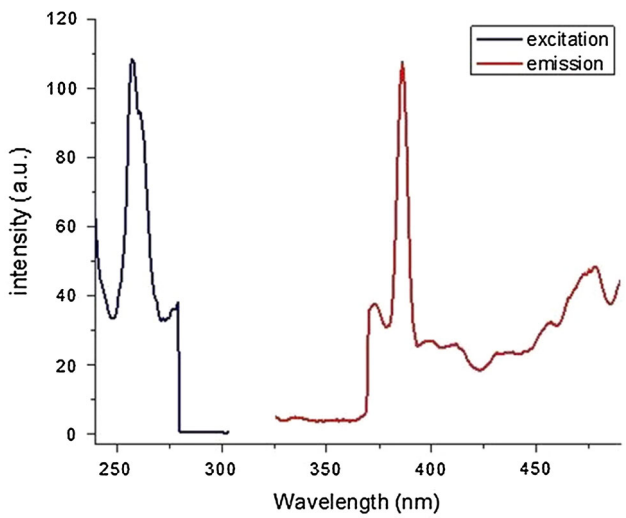

Fig. 6 Photoluminescence spectra for γ-Gd_2S_3 nanoparticles

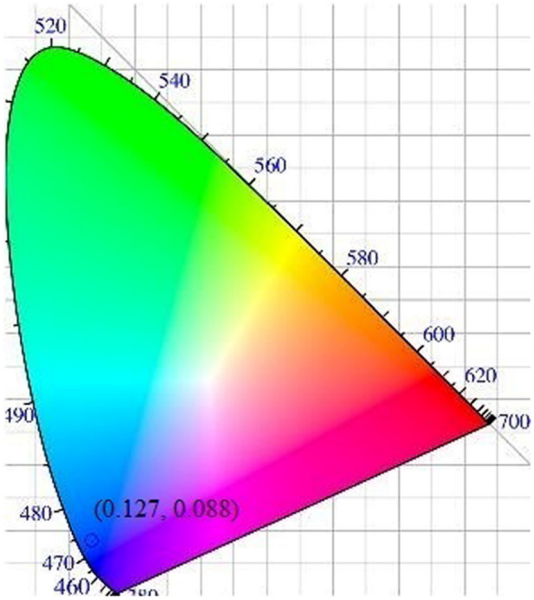

Fig. 7 CIE chromatograph for γ-Gd_2S_3 nanoparticles

Conclusions

In this paper, green ionic liquid-assisted hydrothermal synthesis of γ-Gd_2S_3 nanoparticles has been carried out at low temperature. Ionic liquid [EMIM][$EtSO_4$] was used in the process. Structural and phase analysis was carried out using XRPD studies which suggest a Th_3P_4-type cubic structure and γ-phase for the synthesized nanoparticles. SEM images suggest that the synthesized nanoparticles have cuboidal plate-like morphology which assembles in groups to give flower-like morphology. The calculated particle size by Debye–Scherrer method is 86 nm, whereas observed value by DLS technique was 91 nm. The band gap of as-prepared sample was found 2.95 eV which shows a blue shift when compared to bulk sample according to reported literature which might be due to the pronounced quantum mechanical effect on nanoparticles. Photoluminescence spectra for γ-Gd_2S_3 show a strong emission peak at 385 nm and a broad shoulder at 475 nm when excited at 260 nm, and thus can serve as a blue color producing material for display applications and light emitting diodes.

References

Antonietti M, Kuang D, Smarsly B, Zhou Y (2004) Ionic liquids for convenient synthesis of functional nanoaprticles and other inorganic nanostructures. Angew Chem Int Ed 43:4988–4992

Beaudry BJ, Gschneidner KA Jr (1995) CRC Handbook of Thermoelectrics. In: Rowe DM (ed) CRC Press, Boca Raton pp 339–348

Behboudnia M, Habibi-Yangjeh A, Zafari-tarzanag Y, Khodayari A (2008) Preparation and characterization of monodispersed nanocrystalline ZnS in water-rich [EMIM]$EtSO_4$ ionic liquid using ultrasonic irradiation. J Cryst Growth 310:4544–4548

Dekker R, Klunder DJW, Borreman A, Diemeer MBJ, Wörhoff K, Driessen A, Stouwdam JW, van Veggel FCJM (2004) Stimulated emission and optical gain in LaF3: Nd nanoparticle-doped polymer-based waveguides. Appl Phys Lett 85:6104–6106

Gadzhiev GG, Ismailov SM, Abdullaev KK, Khamidov MM, Omarov ZM (2001) Thermal and electrical properties of gadolinium sulfides at high temperature. High Temp 39:407

Ge L, Jing X-Y, Wang J, Jamil S, Liu Q, Song D-L, Wang J, Xie Y, Yang P-P, Zhang M-L (2010) Ionic liquid-assisted synthesis of CuS nestlike hollow spheres assembled by microflakes using an oil–water interface route. Cryst Growth Des 10:1688–1692

Grzechnik A (1999) Lanthanide polysulfides at high pressure. J Solid State Chem 148:370

Grzechnik A (2001) Stability and optical properties of c-Gd_2S_3 at high pressures. J Alloys Compd 190:317–318

Haibin Y, Jianhui Z, Ruijin YU, Qiang SU (2009) Synthesis of rare earth sulfides and their UV–vis absorption spectra. J Rare Earth 27:308–311

Huber G, Heumann E, Sandrock T, Petermann K (1997) Up-conversion processes in laser crystal. J Lumin 1–3:172–174

Jiang Y, Zhu Y-J (2005) Microwave assisted synthesis of sulfides M_2S_3 (M = Bi, Sb) nanorods using an ionic liquid. J Phys Chem B 109:4361–4364

Jiang J, Yu SH, Yao WT, Ge H, Zhang GZ (2005) Morphogenesis and crystallisation of Bi_2S_3 nanostructures by an ionic liquid-assisted templating route: synthesis, formation mechanism and properties. Chem Mater 17:6094–6100

Jiang Y, Zhu YJ, Cheng GF (2006) Synthesis of Bi_2Se_3 nanosheets by microwave heating using an ionic liquid. Cryst Growth Des 6:2174–2176

Kim F, Connor S, Song H, Kuykendall T, Yang P (2004) Platonic gold nanocrystals. Angew Chem Int Ed 43:3673–3677

Kong DY, Wang ZL, Lin CK, Quan ZW, Li YY, Li CX, Lin J (2007) Biofunctionalization of CeF_3: Tb^{3+} nanoparticles. Nanotechnology 18:075601

Krichevtsov BB (2001) Anisotropy of the linear and quadratic magnetic birefringence in rare-earth semiconductors γ- Ln_2S_3 (Ln = Dy^{3+}, Pr^{3+}, Gd^{3+}, La^{3+}). J Exp Theor Phys 92:830–839

Kuang D, Xu A, Fang Y, Liu H, Frommen C, Fenske D (2003) Surfactant-assisted growth of novel PbS dendritic nanostructures via facile hydrothermal process. Adv Mater 15:1747–1750

Li P, Jie W, Li H (2011) Influences of hot-pressing conditions on the optical properties of lanthanum sulfide ceramics. J Am Ceram Soc 94:1162–1166

Luguev SM, Lugueva NV, Sokolov VV (2000) Heat conductivity of Gd_2S_3 with excess gadolinium. Phys Solid State 42:1045–1048

Markovich G, Collier CP, Henrichs SE, Remacle F, Levine RD, Heath JR (1999) Architectonic quantum dot solids. Acc Chem Res 32:415–423

Ohta M, Hirai S, Kato H, Sokolov VV, Bakovets VV (2009) Thermal decomposition of NH_4SCN for preparation of Ln_2S_3 (Ln = La and Gd) by sufurization. Mater Trans 50:1885–1889

Prashar V, Pandey SK, Pandey AC (2010) Low-temperature synthesis of quantum size gadolinium monosulfide (GdS) nanoparticles and their pathogen capture efficiency. Chem Commun 46:3143–3145

Qiu J, Qiu JB, Higuchi H, Kawamoto Y, Hirao K (1996) Faraday effect of $GaS_{3/2}$-GeS_2-$LaS_{3/2}$-based glasses containing various rare-earth ions. J Appl Phys 80:5297–5300

Shi H, Qi L, Ma L, Cheng H (2003) Polymer-directed synthesis of penniform $BaWO_4$ nanostructures in reverse micelles. J Am Chem Soc 125:3450–3451

Wang W, Wang S-Y, Liu M (2005) Preparation of γ-Gd2S3 films by ultrasonic spray pyrolysis. Mater Chem Phy 94:182–184

Wang F, Zhang Y, Fan X, Wang M (2006) One-pot synthesis of chitosan/LaF_3: Eu^{3+} nanocrystals for bio-applications. Nanotechnology 17:1527–1532

Williamson GK, Hall WH (1953) X-ray broadening from filed aluminium and wolfram. Acta Metall 1:22–31

Witz C, Huguenin D, Lafait J, Dupont S, Theye ML (1996) Comparative optical studies of Ce_2S_3 and Gd_2S_3 compounds. J Appl Phys 79:2038–2042

Xixian L, Lubin MA, Mingming X, Yao F, Min S, Pang T (2012) Preparation of γ-Gd_2S_3 via thermolysis of $Gd[S_2CN(C_4H_8)]_3$-phen coordination. J Rare Earth 30:802–806

Zhang H, Yang D, Li D, Ma X, Li S, Que D (2005) Controllable growth of ZnO microcrystals by a capping-molecule-assisted hydrothermal process. Cryst Growth Des 5:547–550

Zhou Y (2005) Recent advances in ionic liquids for synthesis of inorganic nanomaterials. Curr Nanosci 1:35–42

Zhu YJ, Wang WW, Qi RJ, Hu XL (2004) Microwave-assisted synthesis of single crystalline tellurium nanorods and nanowires in ionic liquids. Angew Chem Int Ed 43:1410–1414